JOURNAL OF BACTERIOLOGY, Jan. 2007, p. 244–253 Vol. 189, No. 1
0021-9193/07/$08.00+0 doi:10.1128/JB.01126-06

Characterization of *lptA* and *lptB*, Two Essential Genes Implicated in Lipopolysaccharide Transport to the Outer Membrane of *Escherichia coli*[▽]

Paola Sperandeo,[1] Rachele Cescutti,[2] Riccardo Villa,[2] Cristiano Di Benedetto,[3] Daniela Candia,[3] Gianni Dehò,[1] and Alessandra Polissi[2]*

Dipartimento di Scienze Biomolecolari e Biotecnologie, Università degli Studi di Milano, Milan, Italy[1]*; Dipartimento di Biotecnologie e Bioscienze, Università di Milano-Bicocca, Milan, Italy*[2]*; and Dipartimento di Biologia, Università degli Studi di Milano, Milan, Italy*[3]

Received 27 July 2006/Accepted 11 October 2006

The outer membrane (OM) of gram-negative bacteria is an asymmetric lipid bilayer that protects the cell from toxic molecules. Lipopolysaccharide (LPS) is an essential component of the OM in most gram-negative bacteria, and its structure and biosynthesis are well known. Nevertheless, the mechanisms of transport and assembly of this molecule in the OM are poorly understood. To date, the only proteins implicated in LPS transport are MsbA, responsible for LPS flipping across the inner membrane, and the Imp/RlpB complex, involved in LPS targeting to the OM. Here, we present evidence that two *Escherichia coli* essential genes, *yhbN* and *yhbG*, now renamed *lptA* and *lptB*, respectively, participate in LPS biogenesis. We show that mutants depleted of LptA and/or LptB not only produce an anomalous LPS form, but also are defective in LPS transport to the OM and accumulate de novo-synthesized LPS in a novel membrane fraction of intermediate density between the inner membrane (IM) and the OM. In addition, we show that LptA is located in the periplasm and that expression of the *lptA-lptB* operon is controlled by the extracytoplasmic σ factor RpoE. Based on these data, we propose that LptA and LptB are implicated in the transport of LPS from the IM to the OM of *E. coli*.

The cell envelope of gram-negative bacteria consists of an inner (IM) and an outer (OM) membrane separated by the periplasmic space, which contains the peptidoglycan layer. The OM is an asymmetric bilayer, with phospholipids in the inner leaflet and lipopolysaccharides (LPS) facing outward (28, 32). LPS, a molecule unique to gram-negative bacteria, consists of the lipid A moiety (a glucosamine-based phospholipid) linked to a short-core oligosaccharide and the distal O-antigen polysaccharide chain. The core oligosaccharide can be further divided into the inner core, composed of 3-deoxy-D-manno-octulosanate (KDO) and heptose, and the outer core, with a somewhat variable structure. *Escherichia coli* K-12 synthesizes a shorter LPS consisting of a lipid A moiety linked to a short-core oligosaccharide but missing the O-antigen chain (28). LPS is essential in most gram-negative bacteria, with the notable exception of *Neisseria meningitidis*. In *E. coli*, the minimal part required for viability consists of the KDO_2 lipid IV_A moiety (28).

LPS is synthesized in the cytoplasmic face of the IM and must traverse the IM and the periplasm to reach its final destination in the outer face of the OM (6, 28). Translocation across the IM requires the ABC transporter MsbA, which mediates the flipping from the inner leaflet (the site of the synthesis) to the outer leaflet of the IM (14, 27, 44). MsbA has also been implicated in phospholipid transport across the IM of *E. coli* (13, 14). Interestingly, MsbA in *N. meningitidis* is not essential and seems not to be required for phospholipid transport (39). How LPS traverses the periplasm and is inserted into the OM is much less understood.

Because of its hydrophobic lipid A moiety, transport of LPS through the aqueous periplasm is thermodynamically unfavorable. In *E. coli*, it has been shown that lipoprotein (Lpp) transport across the periplasmic space is mediated by the LolA chaperone protein. The system is energized by the LolCDE protein complex, an ABC transporter located in the IM. After transport across the periplasm, Lpps are transferred from LolA to the receptor, LolB, in the OM (reviewed in reference 41). No evidence for a similar mechanism has been found so far in the transport of LPS. de Cock and coworkers have recently shown in *E. coli* spheroplasts that de novo-synthesized LPS, unlike Lpps, are not released in the presence of a periplasmic extract. Moreover, the authors showed that LPS cofractionated with remnants of the OM, and this was dependent on the presence of a functional MsbA protein in spheroplasts. These observations have been taken as evidence that transport of LPS could proceed via contact sites between the two membranes (40), thus lending support to earlier proposals that IM-OM adhesion sites (also known as Bayer bridges) could be implicated in LPS transport to the OM (references 2 and 3 and references therein; 16). However, the existence of these points of physical contact between the two membranes has been questioned; they may be artifacts occurring during the cell fixation process used in electron microscopy (17).

A protein implicated in LPS targeting to the OM is Imp, a β-barrel OM protein. Braun and Silhavy demonstrated that Imp is essential in *E. coli* and that its depletion results in abnormalities in OM assembly, with newly synthesized lipids and outer membrane proteins appearing in a novel membrane

* Corresponding author. Mailing address: Dipartimento di Biotecnologie e Bioscienze, Università di Milano-Bicocca, Piazza della Scienza 220126, Milano, Italy. Phone: 39-02-64483431. Fax: 39-02-6448-3450. E-mail: alessandra.polissi@unimib.it.

▽ Published ahead of print on 20 October 2006.

fraction with higher density than the OM (7). Bos and coworkers demonstrated that Imp is required for proper transport of LPS to the cell surface of *N. meningitidis* (5). This conclusion was based upon the loss of surface accessibility by LPS to neuraminidase and loss of lipid A modification by the OM deacylase PagL (5). However, as in this organism it is not possible to separate the IM and OM by sucrose gradient ultracentrifugation, it could not be assessed where LPS accumulates. In agreement with the observation that *N. meningitidis* can survive without LPS, *imp* is not an essential gene in this organism (5). Very recently, the essential *E. coli* lipoprotein RlpB has been shown to interact physically with Imp. RlpB depletion results in defects in OM biogenesis similar to those of Imp depletion, and based on the observation that depletion of both proteins activates the OM enzyme PagP to modify LPS, the authors conclude that the Imp/RlpB complex is responsible for LPS reaching the outer surface of the OM (43).

The OM represents an effective permeability barrier to protect the cells from toxic compounds, such as antibiotics and detergents, thus allowing bacteria to inhabit several different and often hostile environments. The integrity of the extracytoplasmic compartments (the periplasm and OM) is monitored by at least two signaling systems, dependent on Cpx and σ^E, respectively, that sense the status of the cell envelope and respond to repair damage when necessary (reviewed in reference 33). The Cpx system seems to be triggered mainly by damage to surface structures, such as pili (29), whereas the alternative σ^E factor is activated by unfolded envelope proteins and abnormal LPS (20, 23, 38). In agreement with this, genes implicated in cell envelope biogenesis (such as *imp*) or in LPS biosynthesis have been found to belong to the σ^E regulon (7, 10).

We have recently identified two new essential genes of *E. coli*, *yhbN* and *yhbG*, with unknown functions (35). *yhbN* and *yhbG* are the distal genes of a cluster comprising four additional genes. Several lines of evidence obtained in our laboratory implicate these two genes in OM biogenesis: (i) *yhbN* and *yhbG* are both essential and cotranscribed, (ii) they are well conserved in many gram-negative bacteria, (iii) the cluster in which they are organized comprises two genes (*kdsD* and *kdsC*) involved in KDO biosynthesis, and (iv) mutants defective in their expression exhibit altered OM permeability (35).

In this study, we provide evidence that YhbN and YhbG are implicated in the transport of LPS from the inner to the outer membrane of *E. coli*. Henceforth, *yhbN* and *yhbG* will be renamed *lptA* and *lptB* (for *LP*S *t*ransport), respectively.

MATERIALS AND METHODS

Bacterial strains and media. The bacterial strains and plasmids used in this work are listed in Table 1. Oligonucleotide primers are listed in Table 2. Bacteria were grown in either LD broth or M9 minimal medium (18) supplemented with 0.2% glycerol as a carbon source. When required, 0.2% L-arabinose (as an inducer of the *araBp* promoter), 0.2% glucose, 20 μg/ml Casamino Acids, 0.5 mM IPTG (isopropyl-β-D-thiogalactopyranoside), 100 μg/ml ampicillin (Amp), 50 μg/ml kanamycin (Kan), and 25 μg/ml chloramphenicol (Cam) were added. Solid media were as described above with 1% agar.

Construction of mutants BB-10 and BB-11 by allele replacement. Allele replacement was performed using the procedure based on the λ Red recombination system (11). To obtain BB-10 (Table 1), the mutant Δ*rseA1*::*cat* allele was prepared in vitro by a three-step PCR procedure (8) using AP97 and AP98 primers and, as templates, the *cat* cassette (which confers chloramphenicol resistance) amplified by pKD3 using AP79-AP80 primers and two DNA fragments for the flanking homology regions obtained by PCR amplification of *E. coli* MG1655 DNA with oligonucleotides AP95-AP97 and AP96-AP98, respectively (Table 2). Insertion of the *cat* cassette resulted in the removal of amino acid residues 2 to 198 of the 216-codon-long *rseA* coding sequence. To obtain the Δ*rseA1* mutant (BB-11), BB-10 was transformed with pCP20 and ampicillin-resistant transformants were selected at 30°C. Removal of the *cat* cassette, which generated an in-frame deletion replaced by an 18-codon scar (11), was then obtained by colony purification of a few transformants at 43°C and screening them for loss of both Amp and Cam resistance. The presence of the Δ*rseA1* allele in BB-11 was verified by PCR.

TABLE 1. Bacterial strains and plasmids

Strain or plasmid	Relevant characteristics	Source or reference
Strains		
BB-4	BW25113 Φ(*kan araC araBp-yhbN*)*1*	35
BB-5	BW25113 Φ(*kan araC araBp-yhbG*)*1*	35
BB-10	BW25113 Δ*rseA1*::*cat*	This work
BB-11	BW25113 Δ*rseA1*; in-frame deletion by removal of *cat* cassette from BB-10	This work
BW25113	Δ(*araD-araB*)*567* Δ*lacZ4787*(::*rrnB-4*) *lacI*^{q} λ$^-$ *rpoS396*(Am) Δ(*rhaD-rhaB*) *rrnB-4 hsdR514*	11
DH5α	Δ(*argF-lac169*) ϕ80 *dlacZ58*(M15) *glnV44*(AS) λ$^-$ *rfbD1 gyrA96 recA1 endA1 spoT1 thi-1 hsdR17*	15
MG1655	LAM *rph-1*	1
Plasmids		
pGS100	pGZ119EH derivative; contains TIR sequence downstream of *tacp*	35
pGS109	pGS100 *tacp-lptA*-His$_6$	This work
pGS110	pGS100 *tapc-lptB*-His$_6$	This work
pCP20	FLP λ*cI857* λP Rep(Ts) Cam^r Amp^r	9
pKD3	*oriR*γ; Amp^r Cam^r; source of *cat* cassette	11
pKD46	*oriR101 repA101*(Ts) *araC araBp-gam-bet-exo* Amp^r	11
pRS415	pBR322-derived plasmid containing the complete *lac* operon without promoter; Amp^r	34
pRP1	pRS415 derivative containing the σ^E-dependent *lptAp* promoter (297 bp)	This work
pRP2	pRS415 derivative containing the σ^{70}-dependent *yrbGp* promoter (375 bp)	This work

Plasmid construction. Plasmids pGS109 and pGS110 express LptA and LptB, respectively, with a C-terminal His$_6$ tag (LptA-H and LptB-H) upon IPTG induction. They were constructed by PCR amplifying the *lptA* and *lptB* open reading frames from genomic MG1655 DNA with primers AP55-AP64 (*lptA*) or AP56-AP65 (*lptB*) (Table 2). The PCR products were EcoRI-XbaI digested and cloned in pGS100 cut with the same enzymes. The EcoRI-XbaI inserts in the pGS109 and pGS110 were verified by sequencing.

Plasmids pRP1 and pRP2 were constructed by cloning into EcoRI-BamHI-digested pRS415 the *E. coli* chromosomal regions containing the putative *lptAp* and *yrbGp* promoters, respectively. The *lptAp* and *yrbGp* DNAs were PCR amplified from MG1655 genomic DNA using primers AP69-AP70 and AP71-AP72, respectively, and digested with EcoRI-BamHI. The two EcoRI-BamHI inserts in plasmids pRP1 and pRP2 were verified by sequencing.

Total LPS extraction and analysis. Bacterial cultures grown at 37°C in LD-arabinose up to an optical density at 600 nm (OD_{600}) of 0.2 were harvested by centrifugation, washed in LD, and diluted 100-fold in LD with or without arabinose. Samples at a total OD_{600} of 2 were taken at different time points, and LPS was extracted from cell pellets by a mini-phenol-water extraction technique as described previously (30). Briefly, the cells were resuspended in water and pelleted (5 min; 10,000 × *g*) to remove the exopolysaccharides. The pellet was

TABLE 2. Oligonucleotides

Name	5′ to 3′ sequence[a]	Use/description
AP55	cgagagaggaattcaacATGAAATTCAAAACAAACAAACTC	pGS109 construction, with AP64; EcoRI
AP56	cgagaggaattcACCATGGCAACATTAACTGCAAAG	pGS110 construction, with AP65; EcoRI
AP64	gtgatcacatctagatcagtggtggtggtggtggtgATTACCCTTCTTCTGTGCCG	pGS109 construction, with AP55; insertion of C-terminal His_6 tag into LptA; XbaI
AP65	gtgatcacatctagatcagtggtggtggtggtgGAGTCTGAAGTCTTCCCCA	pGS110 construction, with AP56; insertion of C-terminal His_6 tag into LptB; XbaI
AP69	cgagaggaattcGGTCCGTAAAAGCAGATAAAGCC	pRP1 construction, with AP70; EcoRI
AP70	cgacgcggatccATTAAGGCTGAGTTTGTTTG	pRP1 construction, with AP69; BamHI
AP71	cgagaggaattcACCGATGCCCGATGGCCCCA	pRP2 construction, with AP72; EcoRI
AP72	cgacgcggatccCAATTAACAGTGCCGTAG	pRP2 construction, with AP71; BamHI
AP79	GTGTAGGCTGGAGCTGCTTCG	Amplification of *cat* cassette from pKD3 with AP80
AP80	CATATGAATATCCTCCTTAG	Amplification of *cat* cassette from pKD3 with AP79
AP93	GATGTTCAGATTCTGTAGAC	For control of BB-10 and BB-11 mutant regions, with AP94
AP94	CTGAATAATCCGTCGGAATAG	For control of BB-10 and BB-11 mutant regions, with AP93
AP95	gaagcagctccagcctacaCCTAATACCCTTATCCAGTATC	*cat* hybrid primer for BB-10 construction by three-step PCR, with AP97
AP96	ctaaggaggatattcatatggGAACGCAATCGCAGTAA	*cat* hybrid primer for BB-10 construction by three-step PCR, with AP98
AP97	CAGCATAAAGTGGCGAGT	BB-10 construction by three-step PCR, with AP95
AP98	CACGCGAAATTGTTCCAG	BB-10 construction by three-step PCR, with AP96

[a] *E. coli* genomic sequences are in uppercase; restriction sites are underlined and specified in the "Use/description" column.

resuspended in 0.3 ml phosphate buffer, pH 7, and thoroughly vortexed; 0.3 ml of phenol equilibrated with 0.1 M Tris-HCl at pH 5.5 was added, and the suspension was vortexed. The tubes were placed in a 65°C heating block for 15 min with thorough vortexing every 5 min and then cooled in ice. After centrifugation (5 min; 10,000 × *g*), the water phase was removed, dialyzed (2,000-molecular-weight cutoff) against phosphate buffer, pH 7, and dried under vacuum. The lyophilized material was then dissolved in 30 μl of polyacrylamide gel electrophoresis (PAGE) sample buffer. LPS was separated by Tricine–sodium dodecyl sulfate (SDS)-PAGE and silver stained as described previously (36).

***N*-Acetyl[^{3}H]glucosamine pulse-labeling and cell fractionation.** Mutants were grown in LD-arabinose up to an OD_{600} of 0.2 at 37°C in the presence of 0.2% *N*-acetylglucosamine (GlnNAc) to induce GlnNAc uptake. The wild-type strain was grown under the same conditions, except that arabinose was omitted from the medium. Cells were then harvested, washed in LD, diluted 100-fold in fresh medium (50 ml) with or without arabinose, and incubated with aeration at 37°C. [^{3}H]GlnNAc pulse-labeling (see below) of the wild type and mutants grown with arabinose was performed when the cultures reached an OD_{600} of 0.6, whereas depleted cultures grown without arabinose were labeled 1 h after the cells reached their maximal OD_{600} (between 0.4 and 0.6). [^{3}H]GlnNAc pulse-labeling was performed by adding *N*-acetyl[^{3}H]glucosamine (1.6 μCi ml^{-1}) to the culture at 37°C and diluting the culture with 1 volume of the same medium containing 0.8% nonradioactive GlnNAc after 2 min. After a 5-min chase, the cells were chilled in ice and harvested by centrifugation. The inner and outer membranes were separated by discontinuous sucrose density gradient centrifugation of a total membrane fraction obtained by spheroplast lysis as described previously (26). Step gradients were prepared by layering 2 ml each of 50, 45, 40, 35, and 30% sucrose solutions (wt/vol) over a 55% sucrose cushion (0.5 ml).

Fractions (200 μl) were collected from the top of the gradient, and 50 μl each was assayed for NADH oxidase activity (26). The total protein concentration was determined in 10-μl samples of each fraction by the Bradford assay (Bio-Rad) as recommended by the manufacturer. The protein profiles of OmpC, OmpF, and OmpA across the gradient were estimated by separating 20 to 40 μl of each fraction on 12.5% SDS-PAGE and by staining the gels with Coomassie blue. To estimate ^{3}H incorporation, 25 μl of each fraction dissolved in 5 ml scintillation liquid (Ready Safe; Beckman-Coulter) was counted in a liquid scintillation counter (LS6500; Beckman).

Analysis of LPS from gradient fractions. To estimate the LPS contents in the gradient fractions, equal volumes were digested with 6 μg of proteinase K (Sigma) at 60°C for 1 h and then separated by the Tricine–SDS-PAGE procedure as described previously (36). LPS were transferred onto a nitrocellulose membrane (Hybond ECL; GE Healthcare) or a polyvinylidene difluoride microporous membrane (Immobilon-P; Millipore) at 60 V for 2 h in an electroblotting apparatus (PBI). LPS on nitrocellulose membranes were immunodetected using a 1:10,000 dilution of the anti-LPS WN1 222-5 monoclonal antibody (HyCult Biotechnology b.v.). Polyvinylidene difluoride membranes with radiolabeled LPS were scanned with a Beta Imager 2000 (Biospace).

Cellular localization of LptA. Cultures of BW25113 containing plasmid pGS109 were grown in M9 glucose minimal medium up to an OD_{600} of 0.7, and LptA-H was induced for 1 h with 0.5 mM IPTG. Periplasmic, cytoplasmic, inner, and outer membrane fractions were prepared as described previously (25). Equal amounts of proteins from each fraction were fractionated by 12.5% SDS-PAGE. The tagged proteins were detected by Western blotting using monoclonal anti-His_6 antibody (Roche).

β-Galactosidase assay. Overnight cultures of bacterial strains harboring pRP1, pRP2, or pRS415 plasmids in LD at 30°C were diluted 1:100 and grown with aeration up to an OD_{600} of 0.4. The β-galactosidase activity was then determined by the method of Miller (22).

Light microscopy. BB-4 cells grown in LD-arabinose up to an OD_{600} of 0.2 were harvested by centrifugation, washed in LD, and diluted 100-fold in LD with or without arabinose. Growth was monitored by reading the OD_{600}, and samples were taken at different time points. Cells were harvested by centrifugation, washed, and resuspended in phosphate-buffered saline. The cells were imaged with a Leica TCS SP2 confocal microscope coupled to a Leica DMIRE2 inverted microscope. Transmission images were obtained by the Ar laser line at 488 nm through a PL APO 63× oil immersion objective (numerical aperture, 1.4).

Electron microscopy. Bacterial samples obtained as described above were pelleted in Eppendorf tubes, washed with cacodylate buffer (0.2 M, pH 7.4), and fixed with 2% glutaraldehyde in 0.1 M cacodylate buffer. Samples were then postfixed with 1% osmium tetroxide in 0.1 M cacodylate buffer, dehydrated in a graded ethanol series, and embedded in an Epon-Araldite mixture according to standard transmission electron microscopy (TEM) methods (19). Semithin (1-μm) and ultrathin (~50-nm) sections were cut with a Reichert-Jung ULTRACUT E using diamond knives (DIATOME histo and Ultra 45°). Semithin sections, collected on standard slides and stained with crystal violet and basic fuchsin, were controlled under a Jenaval light microscope. Ultrathin sections, collected on 300-mesh copper grids, were stained with aqueous uranyl acetate and lead citrate (31), carbon coated under an EMITECH K400X carbon coater, and observed with a Jeol 100 SX electron microscope. Micrographs were taken directly under the microscope with Kodak 4489 photographic films for TEM.

RESULTS

Expression of *lptA* and *lptB* is controlled by σ^E. Genetic analysis of the *yrbG-lptB* locus indicated that *lptA* and *lptB* are organized in a dicistronic operon, and a putative σ^E-dependent

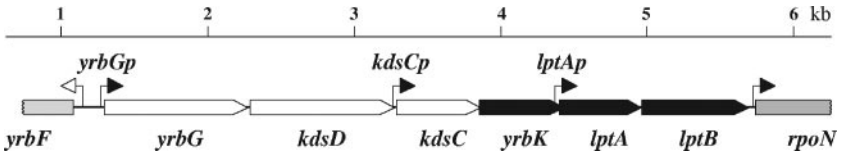

FIG. 1. Organization of the *yrbG-lptB* locus. The open reading frames are drawn to scale as arrowed rectangles (open, nonessential genes; solid, essential genes; gray, truncated flanking genes). Promoters are indicated by bent arrows (open, putative promoters; solid, documented promoters). Coordinates (in kb) on the top bar are from the *E. coli* complete genomic sequence (GenBank NC_000913) after subtracting 3337.

promoter consensus sequence was identified 61 nucleotides upstream of the *lptA* start codon (35) (Fig. 1). To obtain experimental evidence of this putative promoter, we created in the promoter-probe vector pRS415 an *lptAp-lacZ* and, as a control, a *yrbGp-lacZ* translational fusion (pRP1 and pRP2, respectively) (Table 1). The β-galactosidase activity was assessed in BW25113 and its Δ*rseA1* derivative, BB-11 (Table 1). RseA is an anti-σ factor whose loss results in a constitutively high level of σ^E activity (24). The β-galactosidase activity in BB-11 transformed with pRP1 was approximately 10-fold higher than the activity measured in BW25113 transformed with the same plasmid, whereas no variation was observed in both BW25113 and BB-11 harboring either pRP2 or the promoterless vector (Fig. 2). Thus, *lptA* and *lptB* can be expressed from a σ^E-dependent promoter.

LptA is a periplasmic protein. Recently, LptB (YhbG) has been found associated with the plasma membrane (37), whereas nothing was known about the cellular localization of LptA. The *lptA* gene encodes a 185-amino acid protein (predicted mass, 20.13 kDa). Primary sequence analysis revealed a putative N-terminal signal sequence, suggesting that the protein is transported across the IM. Blast homology searches found LptA homologues in all five subclasses of *Proteobacteria* but none in gram-positive bacteria and in *Archea* (http://www.ncbi.nlm.nih.gov/BLAST/). None of these putative proteins has been characterized. To define the subcellular localization of LptA, we constructed a tagged version of the protein carrying a C-terminal His_6 tag (LptA-H) under the control of the IPTG-inducible *tacp* promoter (plasmid pGS109) (Table 1). Ectopic expression of the LptA protein in rich medium was toxic for cells (not shown), and thus, growth and induction with IPTG were performed in M9-glucose minimal medium. Periplasmic, cytoplasmic, inner, and outer membrane fractions from IPTG-induced and noninduced BW25113/pGS109 were prepared as described previously (25) and analyzed by Western blotting using monoclonal anti-His_6 tag antibodies. As shown in Fig. 3, LptA-H was detectable only in the periplasmic fraction.

Morphological and structural abnormalities in LptA-LptB-depleted cells. BB-4 is a conditional-lethal (arabinose-dependent) mutant in which the arabinose-inducible *araBp* promoter drives expression of *lptA* and *lptB* (Table 1). LptA-LptB depletion leads to growth arrest and cell death after six or seven generations (150 min following the shift to a medium lacking arabinose), followed by a modest decline in cell turbidity (35) (Fig. 4A). We thus examined whether LptA-LptB depletion would cause recognizable morphological anomalies in mutant cells. Light microscopy observation showed no difference between depleted and nondepleted cells up to 90 min after the removal of arabinose. At later time points (150 and 210 min), LptA-LptB-depleted cells showed mostly short filaments (Fig. 4B). Furthermore, ultrastructural analysis by TEM allowed us to detect accumulated extra membrane material or multilayered membranous bodies within the periplasmic space and the budding of vesicles derived from the OM (Fig. 4D and E). A similar phenotype has been observed in Imp- and RlpB-depleted cells (43).

We then examined the LPS profile. Total LPS was extracted at 90, 150, and 210 min; fractionated by Tricine–SDS-PAGE; and silver stained. Interestingly, in depleted BB-4 cells late (150 and 210 min) after arabinose removal, an anomalous form of LPS visible as a ladder of bands migrating more slowly than the native LPS was observed (Fig. 4C). In addition, increased levels of LPS seemed to accumulate in the BB-4 mutant 210 min after LptA-LptB depletion (Fig. 4C), as was also observed upon Imp and RlpB depletion (43).

Depletion of LptA and LptB affects LPS transport to the OM. To further investigate the roles of LptA and LptB in LPS maturation, we followed the fate of newly synthesized LPS by

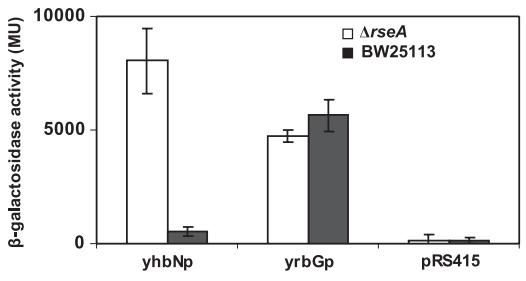

FIG. 2. Promoter activities of *yrbGp* and *lptAp*. The activities of the reporter fusions *yrbGp-lacZ* and *lptAp-lacZ* were assessed in wild-type and Δ*rseA* strains. β-Galactosidase activity measurements were performed in duplicate and calculated in Miller units. The data presented are the averages (with standard deviations) of three independent experiments.

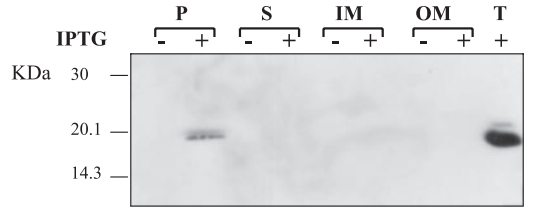

FIG. 3. Subcellular localization of LptA. BW25113 cells containing plasmid pGS109 were induced with IPTG and then fractionated as described in Materials and Methods. P, periplasmic proteins; S, cytoplasmic proteins; IM, solubilized inner membrane proteins; OM, solubilized outer membrane proteins; T, total proteins.

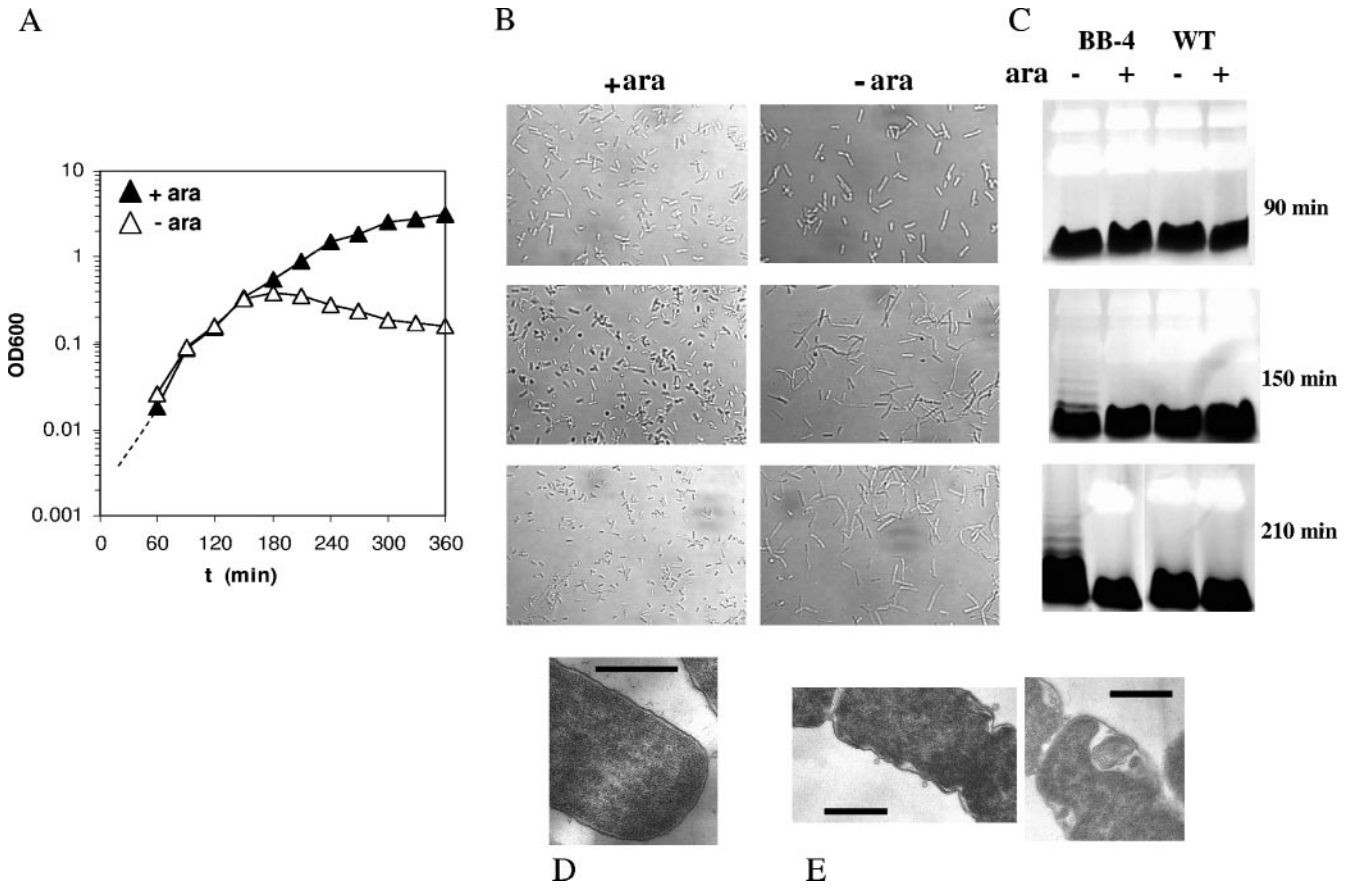

FIG. 4. Growth curve, cell morphology, and LPS profile upon LptA-LptB depletion. (A) Bacterial cultures grown in LD-arabinose up to an OD_{600} of 0.2 were harvested by centrifugation, washed in LD, and diluted 100-fold in LD with arabinose (+ara) or without arabinose (−ara). Growth was monitored by optical density at 600 nm. (B) Light microscopy images of LptA-LptB-depleted (−ara) and nondepleted (+ara) cells taken at different time points. (C) LPS profiles of BB-4 and BW25113 (wild type [WT]) grown with and without arabinose. LPS extracted from cultures with a total OD_{600} of 2 were separated on 18% Tricine–SDS-PAGE and silver stained. The amount of LPS corresponding to an OD_{600} of 0.4 was loaded in each lane. (D and E) Electron microscopy images of wild-type (D) and BB-4 depleted (E) cells. Scale bars, 0.5 μm.

pulse-labeling wild-type, BB-4-depleted, and nondepleted cells with the LPS precursor *N*-acetyl[^{3}H]glucosamine. Membranes were then fractionated by isopycnic sucrose density gradient centrifugation, as described in Materials and Methods. The fractions were assayed for total proteins, NADH oxidase activity as an IM marker, incorporated radioactive precursor (Fig. 5A, C, and E), total LPS, ^{3}H-labeled LPS, and OmpC, OmpF, and OmpA porin profiles (Fig. 5B, D, and F). As shown in Fig. 5A and C, wild-type and nondepleted BB-4 cells displayed a bimodal protein distribution. Most NADH oxidase activity was found in the lighter peak (IM; fractions 15 to 23), whereas the denser peak (OM; fractions 39 to 43) contained most of the total LPS (Fig. 5B and D, LPS) and proteins of 43.3, 39.1, and 37 kDa, corresponding to the masses of OmpC, OmpF, and OmpA porins, respectively, as seen by SDS-PAGE (Fig. 5B and D, OmpC/F-OmpA). The radioactivity in wild-type and nondepleted BB-4 cells was found mainly associated with fractions corresponding to the OM, indicating that *N*-acetyl[^{3}H]glucosamine was readily incorporated into LPS (Fig. 5A and C). Moreover, ^{3}H-labeled LPS were found in fractions 39 to 45, indicating that newly synthesized LPS are transported to the OM (Fig. 5B and D, ^{3}H-LPS).

On the other hand, the fractionation profiles of LptA-LptB-depleted cells were markedly different. Proteins did not display a clear bimodal pattern, and a peak of intermediate density containing mostly NADH oxidase activity appeared (Fig. 5E, heavy IM [hIM], fractions 29 to 33). The major amount of LPS was found in fractions denser than the hIM (fractions 33 to 43). However, the distribution of LPS was skewed toward lower densities than those found in wild-type and nondepleted cells. These data seem to indicate that a substantial fraction of the IM and OM cannot be cleanly separated by buoyant-density centrifugation. This is further supported by the distribution of OmpC/F-OmpA proteins, which were detected by SDS-PAGE in fractions 33 to 41, thus floating at a density lower than the OM (Fig. 5F, OmpC/F-OmpA).

Interestingly, a substantial amount of the abnormal form of high-molecular-weight LPS could be detected in fractions 15 to 27 and was thus lighter than hIM. In the denser fractions, however, the presence of the abnormal LPS could be masked by the strong LPS signal. Moreover the distribution of radioactivity was found mainly associated with the hIM peak of intermediate density (Fig. 5E, fractions 29 to 33). Finally, as expected from the radioactivity profile, most of de novo-syn-

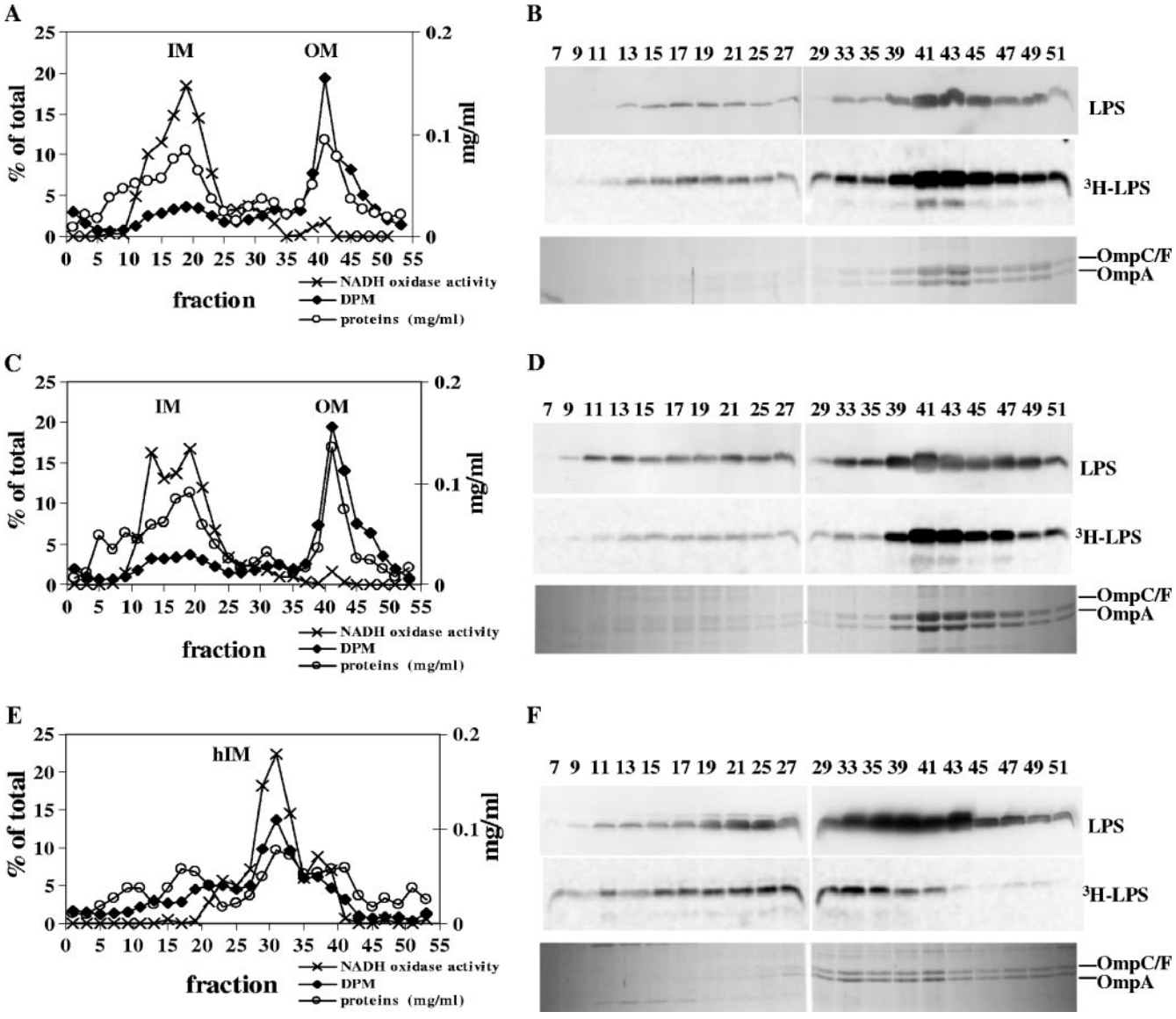

FIG. 5. Membrane fractionation and LPS profile of LptA-LptB-depleted mutant. BB-4 mutant cells shifted to an arabinose-free medium were pulse-labeled for 2 min with [^{3}H]GlnNAc 1 hour after they had reached their maximal OD_{600} (about 0.5 to 0.6) and then harvested by centrifugation 5 min after the chase; the nondepleted and wild-type cultures were pulse-labeled when they reached the same OD_{600}, as described in Materials and Methods. Total membranes prepared from cells were fractionated into inner and outer membranes by sucrose density gradient centrifugation. Fractions of 200 μl were collected from the top of the gradient and analyzed for total protein content, NADH oxidase activity, OmpC/F-OmpA protein profiles, and total and labeled LPS. (A, C, and E) Membrane fractionation profiles of BW25113, nondepleted BB-4, and LptA-LptB-depleted BB-4 cells, respectively. NADH oxidase activity (×) and disintegration per minutes (DPM; black diamonds) are expressed as percentages of the total. Total proteins (open circles), determined with the Bio-Rad Bradford assay, are expressed in mg/ml. (B, D, and F) LPS profiles of BW25113, nondepleted BB-4, and LptA-LptB-depleted BB-4 cells, respectively. LPS, LPS profiles of fractions determined by Western blotting using anti-LPS WN1 222-5 monoclonal antibody; ^{3}H-LPS, newly synthesized radiolabeled LPS scanned with a β-imager; OmpC/F-OmpA, profiles of the major OM porins.

thesized LPS fractionated in the lighter part of the gradient corresponding to IM and hIM peaks, whereas little label was detected in heavier fractions (Fig. 5F, ^{3}H-LPS). These data indicate that LptA-LptB depletion results in a dramatic alteration of both the IM and the OM and that under these conditions, newly synthesized LPS are not transported to the OM.

Both LptA and LptB are implicated in LPS transport to the OM. The experiments described above show that repression of the *lptA-lptB* operon impairs LPS transport and OM biogenesis. We thus tested whether each gene is implicated in this process by analyzing the LPS-incorporated radioactivity profile in an *N*-acetyl[^{3}H]glucosamine pulse-chase/membrane fractionation experiment, as described above, in cultures individually depleted of either LptA or LptB. LptB depletion was achieved in BB-5 (*araBp-lptB*), in which the expression of *lptB* is arabinose dependent (35), whereas for depletion of LptA, we complemented BB-4 (*araBp-lptA-lptB*) with pGS110, a plasmid that expresses LptB-H (i.e.,

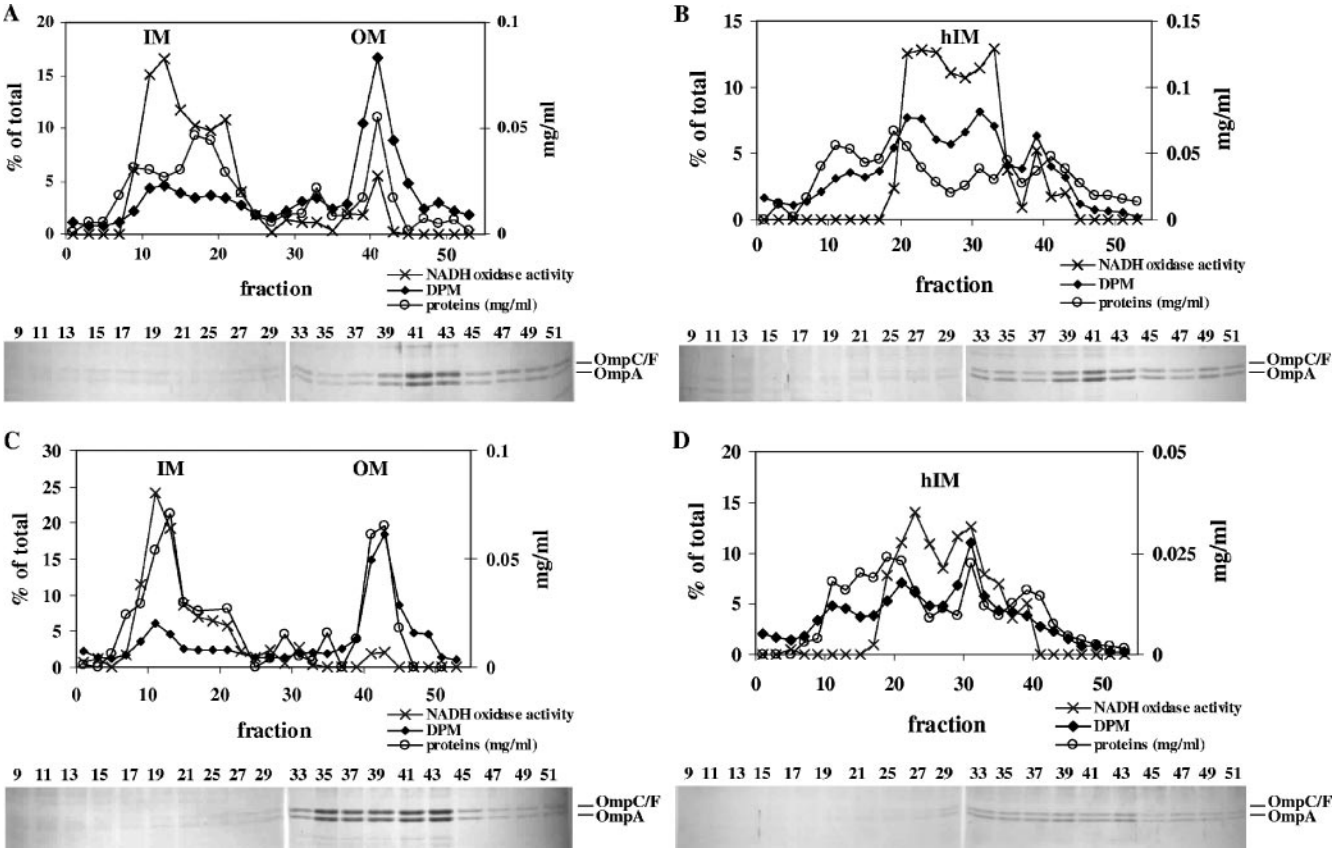

FIG. 6. Membrane fractionation of LptA- or LptB-depleted cells. BB-4/pGS110 and BB-5 mutant cells shifted to an arabinose-free medium were pulse-labeled for 2 min with [^{3}H]GlnNAc 1 hour after they had reached their maximal OD_{600} (about 0.4 to 0.6) and then harvested by centrifugation 5 min after the chase; the nondepleted cultures were pulse-labeled when they reached the same OD_{600}, as described in Materials and Methods. Total membranes prepared from cells were fractionated into inner and outer membranes by sucrose density gradient centrifugation. Fractions of 200 μl were collected from the top of the gradient and analyzed for total protein content, NADH oxidase activity, radioactivity profiles, and OmpC/F-OmpA protein profiles. (A and B) Membrane fractionation profiles and the profiles of the major OM porins (OmpC/F-OmpA) of nondepleted and depleted BB-5 cells, respectively. (C and D) Membrane fractionation profiles and the profiles of the major OM porins (OmpC/F-OmpA) of nondepleted and depleted BB-4/pGS110 cells, respectively. NADH oxidase activity (×) and disintegrations per minutes (DPM; black diamonds) are expressed as percentages of the total. Total proteins (open circles), determined with the Bio-Rad Bradford assay, are expressed in mg/ml.

with a C-terminal His_6 tag) (Table 1). pGS110 was able to complement the arabinose dependence of BB-5, even in the absence of IPTG (data not shown), indicating that the LptB-H is functional and sufficiently expressed even in the absence if the inducer.

When membranes were separated from nondepleted BB-5 and BB-4/pGS110, the fractionation profiles were very similar to those seen in BW25113 or in nondepleted BB-4 cells. As judged by the NADH oxidase activity profile, the IM sedimented around fractions 11 to 19 in both mutants (Fig. 6A and C, top), whereas, based on both total-protein and porin profiles, OM equilibrated around fractions 39 to 43 (Fig. 6A and C, top and bottom). The distribution of radioactivity in BB-5 and BB-4/pGS110 nondepleted cells was found mainly associated with the fractions corresponding to the OM (Fig. 6A and C, top), indicating that the newly synthesized LPS is transported to the OM. On the other hand, when either LptA or LptB was depleted, the fractionation profile resembled that observed in BB-4 depleted cells. Most of the NADH oxidase activity appeared in a peak of intermediate density (hIM fractions 21 to 31 and 21 to 33 in BB4/pGS110 and BB-5, respectively). Although the total-protein profile did not display a clear bimodal pattern, a small peak around fractions 39 to 41 with a density corresponding to the OM and containing porins appeared in both BB4/pGS110 and BB-5 (Fig. 6B and D, top). However, in both depleted mutants, the distribution of porins was skewed toward lower densities than those found in nondepleted cells (Fig. 6B and D, bottom). Interestingly, the radioactivity was found to be associated mainly with the peak of intermediate density in both mutants (fractions 21 to 31 and 21 to 33 in BB4/pGS110 and BB-5, respectively), and very little radioactivity was found in the fractions corresponding to the OM, thus indicating that most of the de novo-synthesized LPS are not transported to the OM.

Overall, these data indicate that depletion of either *lptA* or *lptB* is sufficient to cause a dramatic alteration of both the IM and OM with concomitant impairment of LPS targeting to the OM, and thus, both genes seem to act in the same pathway of LPS transport across the periplasmic space.

DISCUSSION

In this work, we implicate the *E. coli* essential genes *lptA* and *lptB* in LPS transport across the periplasm. We show that the two genes are expressed from a σ^E-dependent promoter. The σ^E regulon responds to envelope stress and is specifically activated by both misfolded OM proteins and alteration of LPS structure (33, 38). Among the target genes whose expression is upregulated by σ^E, there are factors implicated in OM biogenesis. These include Imp, with a postulated role in LPS assembly in the OM (7); SurA, a periplasmic chaperone necessary for proper OM protein folding (7, 10); and YaeT, YfgL, YfiO, and NlpB, which form a multiprotein complex required for OM protein assembly (32). In the *yrbG-lptB* locus, two additional promoters, *kdsCp* and the σ^{70}-dependent *yrbGp*, are predicted upstream of *lptAp* (35; this work) (Fig. 1), and we cannot rule out the possibility that the *lptA* and *lptB* genes may also be expressed from these upstream promoters. However, the presence of a σ^E-dependent promoter places *lptA* and *lptB* in the growing family of genes with extracytoplasmic functions.

We demonstrated that upon LptA-LptB depletion, [^{3}H]GlcNAc, a compound that is normally incorporated into the LPS outer core, accumulates in a novel membrane fraction with higher density than the IM (hIM) and is not transported to the OM. Moreover, in depleted cells, ^{3}H-LPS fractionates with the hIM fraction and is absent in denser fractions (Fig. 5). Similar defects are observed in cells in which LptA and LptB are individually depleted (Fig. 6), indicating that both proteins are required for LPS targeting to the OM. Electron micrographs of LptA-LptB-depleted cells also show serious envelope defects resembling those observed upon Imp or RlpB depletion (43). These data suggest that LptA and LptB are OM biogenesis factors implicated in LPS transport.

We do not know the nature of the hIM peak appearing upon LptA-LptB depletion. A likely hypothesis is that LPS accumulates in the IM, increasing the LPS/phospholipid ratio and thus increasing the density of the IM fraction, whereas conversely, the blockade of LPS transport across the periplasm may result in decreased density of the OM. The behavior of LptA-LptB-depleted cells is reminiscent of Imp and RlpB depletion, where newly synthesized lipids and proteins accumulated in a novel membrane fraction with increased density over that of the OM, which has been taken as evidence of an increased LPS/phospholipid ratio (7, 43). Alternatively, the blockade of the LPS transport machinery may cause abnormal membrane aggregations, as was also observed by electron microscopy, that prevent a clean separation of the IM and OM through sucrose gradient centrifugation.

LPS accumulation in LptA-LptB- and Imp-RlpB-depleted cells suggests that the rate of LPS transport is not coupled to the rate of its synthesis. Interestingly a similar observation was made by Meredith and coworkers, who found that in a mutant unable to synthesize KDO, thus producing only lipid IV_A, the rate of lipid IV_A transport had become uncoupled from its rate of synthesis (21). However, LPS accumulation and changes in membrane fractionation profiles have not been observed upon MsbA depletion or thermal inactivation of a temperature-sensitive *msbA* allele (13, 27, 44). It is possible, however, that this difference could be imputed to different experimental conditions (e.g., incubation under nonpermissive conditions was not long enough for this to occur).

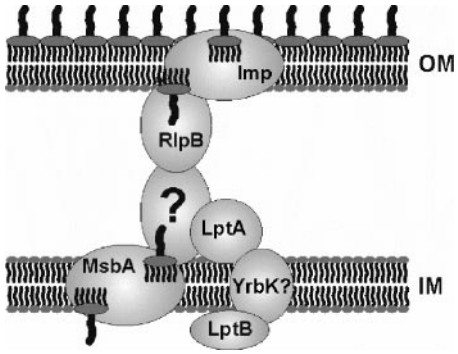

FIG. 7. A model for the transport of LPS. LPS (dark ovals with six small wavy lines, lipid A; larger wavy line, core oligosaccharide) is synthesized in the cytoplasm and flipped over the IM by MsbA. LptA and LptB are part of a protein machine that transports LPS across the periplasm to the OM. A transmembrane component (YrbK?) is postulated to complete the IM-bound ABC transporter. Additional proteins (?) could be part of the complex. The Imp/RlpB complex is thought to mediate the insertion of the newcomer LPS into the OM.

The pulse-labeling experiments with LptA-LptB-depleted cells using [^{3}H]GlcNAc were unable to distinguish the topology of LPS in the hIM peak. However, based on the published data on MsbA-dependent LPS translocation, we hypothesize that in the LptA-LptB-depleted mutants, LPS accumulates in the outer leaflet of the IM. This is consistent with the electron microscopy observation of extra membrane accumulated in the periplasmic space, as was also observed in RlpB- and Imp-depleted mutants (43).

LptA-LptB-depleted cells produce an abnormal, higher-molecular-weight form of LPS that can be detected both in total extracts and in fractionated membranes. Following translocation across the IM, the KDO_2 lipid IV_A moiety with the core sugars attached may undergo additional chemical modifications either in the periplasm or in the OM (4, 42). In the periplasm, the covalent modification of lipid A with the cationic sugar 4-amino-4-deoxy-L-arabinose catalyzed by ArnT is induced by environmental stimuli or appropriate point mutations and leads to polymyxin resistance (42). The anomalous LPS produced upon LptA-LptB depletion could be the result of such chemical modifications occurring when the molecule stacks in the IM facing the periplasm. Further analysis will test this hypothesis.

LptA, as suggested by its amino acid sequence analysis, is a periplasmic protein (Fig. 3) predicted to work with LptB, a protein belonging to the superfamily of ABC transporters (http://ecocyc.org/). Amino acid sequence analysis suggests that the 26.6-kDa LptB protein is soluble and possesses the ATP binding fold, but not the transmembrane domain. However, LptB has been recently identified in the IM in a complex of ~140 kDa, although no interacting partners could be detected (37). We suggest (see the model in Fig. 7) that LptA and LptB, together with an as-yet-unidentified transmembrane partner, may form a membrane-associated complex required for LPS transport, possibly by providing the required energy. A transmembrane partner candidate is YrbK, an essential protein encoded by the gene immediately

upstream in the *yrbG-lptB* locus (Fig. 1) and predicted to be membrane associated (35).

Two main scenarios for the transit of LPS between the IM and the OM have been proposed: transit at sites of contact between the IM and the OM (12, 40) and chaperone-mediated transport through the periplasm (32). Transport of Lpp to the OM proceeds via the latter mechanism, mediated by the periplasmic chaperone LolA and the ABC transporter LolCDE (41). The former mechanism has been postulated for LPS transport based on the observation that Lpp, but not LPS, could be released from spheroplasts in the presence of periplasmic extracts (40). The data presented in this work do not favor either hypothesis.

Overall, our data are consistent with the LPS biogenesis model shown in Fig. 7. LPS synthesized in the inner leaflet of the IM is flipped to the outer leaflet by MsbA. LPS may be escorted through the periplasm by a dedicated chaperone machine that includes LptA, with the system energized by the IM protein complex containing LptB and, possibly, YrbK. Imp, RlpB, and possibly additional proteins could then function in receiving and assembling LPS at the OM.

ACKNOWLEDGMENTS

We are grateful to Alessandro Prinetti for his help with the Beta-Imager analysis. We also thank Anna Villa for help with light microscopy analyses.

This work was initially supported by joint grants from the "Ministero dell'Istruzione, dell'Università e della Ricerca" and the "Università degli Studi di Milano" (Programmi di Rilevante Interesse Nazionale 2002 and FIRB 2001).

REFERENCES

1. **Bachmann, B. J.** 1987. Derivatives and genotypes of some mutant derivatives of *Escherichia coli* K12, p. 1191–1219. *In* J. L. Ingraham, K. B. Low, B. Magasanik, M. Schaechter, and H. E. Umbarger (ed.), *Escherichia coli* and *Salmonella typhimurium*: cellular and molecular biology. ASM Press, Washington, D.C.
2. **Bayer, M. E.** 1968. Areas of adhesion between wall and membrane of *Escherichia coli*. J. Gen. Microbiol. **53:**395–404.
3. **Bayer, M. E.** 1991. Zones of membrane adhesion in the cryofixed envelope of *Escherichia coli*. J. Struct. Biol. **107:**268–280.
4. **Bishop, R. E., H. S. Gibbons, T. Guina, M. S. Trent, S. I. Miller, and C. R. Raetz.** 2000. Transfer of palmitate from phospholipids to lipid A in outer membranes of gram-negative bacteria. EMBO J. **19:**5071–5080.
5. **Bos, M. P., B. Tefsen, J. Geurtsen, and J. Tommassen.** 2004. Identification of an outer membrane protein required for the transport of lipopolysaccharide to the bacterial cell surface. Proc. Natl. Acad. Sci. USA **101:**9417–9422.
6. **Bos, M. P., and J. Tommassen.** 2004. Biogenesis of the Gram-negative bacterial outer membrane. Curr. Opin. Microbiol. **7:**610–616.
7. **Braun, M., and T. J. Silhavy.** 2002. Imp/OstA is required for cell envelope biogenesis in *Escherichia coli*. Mol. Microbiol. **45:**1289–1302.
8. **Chaveroche, M. K., J. M. Ghigo, and C. d'Enfert.** 2000. A rapid method for efficient gene replacement in the filamentous fungus *Aspergillus nidulans*. Nucleic Acids Res. **28:**e97.
9. **Cherepanov, P. P., and W. Wackernagel.** 1995. Gene disruption in *Escherichia coli*: TcR and KmR cassettes with the option of Flp-catalyzed excision of the antibiotic-resistance determinant. Gene **158:**9–14.
10. **Dartigalongue, C., D. Missiakas, and S. Raina.** 2001. Characterization of the *Escherichia coli* sigma E regulon. J. Biol. Chem. **276:**20866–20875.
11. **Datsenko, K. A., and B. L. Wanner.** 2000. One-step inactivation of chromosomal genes in *Escherichia coli* K-12 using PCR products. Proc. Natl. Acad. Sci. USA **97:**6640–6645.
12. **Doerrler, W. T.** 2006. Lipid trafficking to the outer membrane of Gram-negative bacteria. Mol. Microbiol. **60:**542–552.
13. **Doerrler, W. T., H. S. Gibbons, and C. R. Raetz.** 2004. MsbA-dependent translocation of lipids across the inner membrane of *Escherichia coli*. J. Biol. Chem. **279:**45102–45109.
14. **Doerrler, W. T., M. C. Reedy, and C. R. Raetz.** 2001. An *Escherichia coli* mutant defective in lipid export. J. Biol. Chem. **276:**11461–11464.
15. **Hanahan, D.** 1983. Studies on transformation of *Escherichia coli* with plasmids. J. Mol. Biol. **166:**557–580.
16. **Ishidate, K., E. S. Creeger, J. Zrike, S. Deb, B. Glauner, T. J. MacAlister, and L. I. Rothfield.** 1986. Isolation of differentiated membrane domains from *Escherichia coli* and *Salmonella typhimurium*, including a fraction containing attachment sites between the inner and outer membranes and the murein skeleton of the cell envelope. J. Biol. Chem. **261:**428–443.
17. **Kellenberger, E.** 1990. The 'Bayer bridges' confronted with results from improved electron microscopy methods. Mol. Microbiol. **4:**697–705.
18. **Kunz, D. A., and P. J. Chapman.** 1981. Catabolism of pseudocumene and 3-ethyltoluene by *Pseudomonas putida* (*arvilla*) mt-2: evidence for new functions of the TOL (pWWO) plasmid. J. Bacteriol. **146:**179–191.
19. **Maunnsbach, A. B., and B. A. Afzelius.** 1999. Biomedical electron microscopy. Academic Press, London, United Kingdom.
20. **Mecsas, J., P. E. Rouviere, J. W. Erickson, T. J. Donohue, and C. A. Gross.** 1993. The activity of sigma E, an *Escherichia coli* heat-inducible sigma-factor, is modulated by expression of outer membrane proteins. Genes Dev. **7:**2618–2628.
21. **Meredith, T. C., P. Aggarwal, U. Mamat, B. Linder, and R. W. Woodard.** 2006. Redefining the requisite lipopolysaccharide structure in *Escherichia coli*. ACS Chem. Biol. **1:**33–42.
22. **Miller, J. H.** 1992. A short course in bacterial genetics: a laboratory manual and handbook for *Escherichia coli* and related bacteria. Cold Spring Harbor Laboratory Press, Cold Spring Harbor, NY.
23. **Missiakas, D., J. M. Betton, and S. Raina.** 1996. New components of protein folding in extracytoplasmic compartments of *Escherichia coli* SurA, FkpA and Skp/OmpH. Mol. Microbiol. **21:**871–884.
24. **Missiakas, D., M. P. Mayer, M. Lemaire, C. Georgopoulos, and S. Raina.** 1997. Modulation of the *Escherichia coli* σE (RpoE) heat-shock transcription-factor activity by the RseA, RseB and RseC proteins. Mol. Microbiol. **24:**355–371.
25. **Oliver, D. B., and J. Beckwith.** 1982. Regulation of a membrane component required for protein secretion in *Escherichia coli*. Cell **30:**311–319.
26. **Osborn, M. J., J. E. Gander, E. Parisi, and J. Carson.** 1972. Mechanism of assembly of the outer membrane of *Salmonella typhimurium*. Isolation and characterization of cytoplasmic and outer membrane. J. Biol. Chem. **247:**3962–3972.
27. **Polissi, A., and C. Georgopoulos.** 1996. Mutational analysis and properties of the *msbA* gene of *Escherichia coli*, coding for an essential ABC family transporter. Mol. Microbiol. **20:**1221–1233.
28. **Raetz, C. R., and C. Whitfield.** 2002. Lipopolysaccharide endotoxins. Annu. Rev. Biochem. **71:**635–700.
29. **Raivio, T. L., and T. J. Silhavy.** 1999. The σE and Cpx regulatory pathways: overlapping but distinct envelope stress responses. Curr. Opin. Microbiol. **2:**159–165.
30. **Reuhs, B. L., R. W. Carlson, and J. S. Kim.** 1993. *Rhizobium fredii* and *Rhizobium meliloti* produce 3-deoxy-D-manno-2-octulosonic acid-containing polysaccharides that are structurally analogous to group II K antigens (capsular polysaccharides) found in *Escherichia coli*. J. Bacteriol. **175:**3570–3580.
31. **Reynolds, E. S.** 1963. The use of lead citrate at high pH as an electron opaque stain in electron microscopy. J. Cell Biol. **17:**208–212.
32. **Ruiz, N., D. Kahne, and T. J. Silhavy.** 2006. Advances in understanding bacterial outer-membrane biogenesis. Nat. Rev. Microbiol. **4:**57–66.
33. **Ruiz, N., and T. J. Silhavy.** 2005. Sensing external stress: watchdogs of the *Escherichia coli* cell envelope. Curr. Opin. Microbiol. **8:**122–126.
34. **Simons, R. W., F. Houman, and N. Kleckner.** 1987. Improved single and multicopy *lac*-based cloning vectors for protein and operon fusions. Gene **53:**85–96.
35. **Sperandeo, P., C. Pozzi, G. Deho, and A. Polissi.** 2006. Non-essential KDO biosynthesis and new essential cell envelope biogenesis genes in the *Escherichia coli yrbG-yhbG* locus. Res. Microbiol **157:**547–558.
36. **Sprott, G. D., S. F. Kova, and C. A. Schnaitman.** 1994. Cell fractionation, p. 72–103. *In* P. Gerhardt, R. G. E. Murray, W. A. Wood, and N. R. Krieg (ed.), Methods for general and molecular bacteriology. ASM Press, Washington, D.C.
37. **Stenberg, F., P. Chovanec, S. L. Maslen, C. V. Robinson, L. L. Ilag, G. von Heijne, and D. O. Daley.** 2005. Protein complexes of the *Escherichia coli* cell envelope. J. Biol. Chem. **280:**34409–34419.
38. **Tam, C., and D. Missiakas.** 2005. Changes in lipopolysaccharide structure induce the σ^E-dependent response of *Escherichia coli*. Mol. Microbiol. **55:**1403–1412.
39. **Tefsen, B., M. P. Bos, F. Beckers, J. Tommassen, and H. de Cock.** 2005. MsbA is not required for phospholipid transport in *Neisseria meningitidis*. J. Biol. Chem. **280:**35961–35966.
40. **Tefsen, B., J. Geurtsen, F. Beckers, J. Tommassen, and H. de Cock.** 2005. Lipopolysaccharide transport to the bacterial outer membrane in spheroplasts. J. Biol. Chem. **280:**4504–4509.
41. **Tokuda, H., and S. Matsuyama.** 2004. Sorting of lipoproteins to the outer membrane in *Escherichia coli.* Biochim. Biophys. Acta **1694:**IN1–IN9.

42. **Trent, M. S., A. A. Ribeiro, S. Lin, R. J. Cotter, and C. R. Raetz.** 2001. An inner membrane enzyme in *Salmonella* and *Escherichia coli* that transfers 4-amino-4-deoxy-L-arabinose to lipid A: induction on polymyxin-resistant mutants and role of a novel lipid-linked donor. J. Biol. Chem. **276:**43122–43131.
43. **Wu, T., A. C. McCandlish, L. S. Groenberger, S. S. Chng, T. J. Silhavy, and D. Kahne.** 2006. Identification of a protein complex that assembles lipopolysaccharide in the outer membrane of *Escherichia coli*. Proc. Natl. Acad. Sci. USA **103:**11754–11759.
44. **Zhou, Z., K. A. White, A. Polissi, C. Georgopoulos, and C. R. Raetz.** 1998. Function of *Escherichia coli* MsbA, an essential ABC family transporter, in lipid A and phospholipid biosynthesis. J. Biol. Chem. **273:**12466–12475.